Tan *et al. Applied Biological Chemistry* (2022) 65:23
https://doi.org/10.1186/s13765-022-00693-y

KSABC
The Korean Society for Applied Biological Chemistry

ARTICLE

Open Access

Propofol suppresses non-small cell lung cancer progression by modulating circ_0001727/miR-516b-5p/LRRC1 axis

Ming Tan[1], Xin Zhang[1] and Maohui Xing[2*]

Abstract

Background: Propofol plays an anti-cancer role in diverse cancers, including non-small cell lung cancer (NSCLC). We aimed to study the function and underlying mechanism of propofol in NSCLC.

Methods: Cell Counting Kit-8 (CCK-8) and colony formation assays were used to detect cell proliferation. The expression of circ_0001727, microRNA-516b-5p (miR-516b-5p) and leucine-rich repeat-containing protein 1 (LRRC1) mRNA was tested via quantitative real-time polymerase chain reaction (qRT-PCR). Cell migration and invasion were assessed by transwell assay. Angiogenesis and cell apoptosis were determined by tube formation assay and flow cytometry, respectively. Western blot (WB) assay was performed to measure all protein levels. In vivo experiments were conducted via establishing mice xenograft model. Dual-luciferase reporter and RNA Immunoprecipitation (RIP) assays were carried out to verify the relationship between miR-516b-5p and circ_0001727 or LRRC1.

Results: Circ_0001727 was overexpressed in NSCLC, and propofol treatment reduced circ_0001727 level in NSCLC cells. Propofol could repress proliferation, migration, invasion, and angiogenesis while accelerated apoptosis of NSCLC cells, while these effects were augmented by circ_0001727 knockdown. Moreover, circ_0001727 depletion in combined with propofol also inhibited tumorigenesis in vivo. MiR-516b-5p was targeted by circ_0001727, and miR-516b-5p downregulation counteracted the suppressive influence of circ_0001727 deficiency on the malignant behaviors of NSCLC cells. LRRC1 was targeted by miR-516b-5p, and miR-516b-5p exerted its anti-tumor function in NSCLC cells by targeting LRRC1. Additionally, circ_0001727 regulated LRRC1 expression via sponging miR-516b-5p.

Conclusion: Propofol inhibited NSCLC progression by regulation of circ_0001727/miR-516b-5p/LRRC1 axis, which might offer an effective therapeutic target for NSCLC therapy.

Keywords: Non-small cell lung cancer, Propofol, circ_0001727, miR-516b-5p, LRRC1

Introduction

Lung cancer is the most commonly diagnosed cancer in most countries and has become the leading cause of tumor-associated death in 2020 [1]. Non-small cell lung cancer (NSCLC) is a main type of lung cancer [2]. Although great progress has been achieved in therapeutic over the past few decades, and cancer-related death in patients with NSCLC is still high [3]. Therefore, identifying new biomarkers and molecular targets is essential for improving the survival of NSCLC patients.

Propofol is a frequently used intravenous anesthetic during tumor resection because of its rapid recover, short action, and little side effect [4]. Propofol has an anti-cancer role in various types of cancer, such as bladder [5], pancreatic [6], liver [7], and colorectal cancers [8]. In addition, propofol also suppresses NSCLC cell proliferation and induces apoptosis [9]. Considering that propofol

*Correspondence: 18971891725@163.com
[2] Department of Oncology, The Central Hospital of Enshi Tujia and Miao Autonomous Prefectrue, No. 156 Wuyang Avenue, Enshi City 445000, Hubei, China
Full list of author information is available at the end of the article

can be widely used in clinical surgery, it is critical to study the relationship between propofol and NSCLC and determine the underlying mechanism.

As a new kind of non-coding RNAs (ncRNAs), circular RNAs (circRNAs) have become the latest focus of RNA research [10, 11]. It is acknowledged that circRNAs have no 5′-cap and 3′-end poly A tail and are able to form covalent closed structures, making circRNAs very stable and highly resistant to RNase R [12, 13]. Recently, growing evidence has revealed the importance of circRNAs in a variety of diseases, including cancers [14, 15]. Some circRNA are involved in the initiation and development of NSCLC [16–18]. Circ_0001727 (also known as circ-ZKSCAN1), a circRNA derived from ZKSCAN1 gene, has been reported to promote NSCLC development [19]. However, whether circ_0001727 is involved in propofol-mediated effect in NSCLC remains unclear.

MicroRNAs (miRNAs) are short (~22 nt) ncRNAs that can regulate gene expression [20]. Many miRNAs can function as tumor suppressors or facilitators in many cancers [21]. Recently, the connection between miRNAs and circRNAs has attracted great attention. One popular hypothesis shows that circRNAs can competitively bind to miRNA response elements to function as miRNA sponges, thereby regulating target gene expression [22]. A former report declared that miR-516b-5p could inhibit NSCLC progression [23]. In NSCLC, leucine-rich repeat-containing protein 1 (LRRC1) has been reported to serve as an oncogene [24]. However, the interactions among circ_0001727, miR-516b-5p, LRRC1 in NSCLC development and propofol-mediated functions have not been reported.

A549 cell line was initiated in 1972 by D.J. Giard, et al. through explant culture of lung carcinomatous tissue from a 58-year-old Caucasian male. H1299 cell line was established from a lymph node metastasis of the lung from a NSCLC patient who had received prior radiation therapy. In our work, the function of propofol in NSCLC cells (A549 and H1299) was studied. Further, we also investigated the interaction between propofol and circ_0001727/miR-516b-5p/LRRC1 axis. The purpose of this research to provide a novel insight into the use of anesthetics for the treatment of NSCLC.

Materials and methods

Specimen collection

NSCLC tissue specimens (n = 30) and matched nearby normal tissues (n = 30) were obtained from NSCLC patients after surgical resection at the Central Hospital of Enshi Tujia and Miao Autonomous Prefectrue. All patients signed their written informed consents. With approval from the Research Ethics Committee of the Central Hospital of Enshi Tujia and Miao Autonomous Prefectrue, the current study was conducted.

Cell culture and transfection

NSCLC cells (A549 and H1299) and normal lung epithelial cells (BEAS-2B) were obtained from COBIOER (Nanjing, China). DMEM (Invitrogen, Carlsbad, CA, USA) that contained FBS (Invitrogen) was used for culturing BEAS-2B and NSCLC cells in standard conditions (5% CO_2, 37 ℃). For treatment of propofol, cells were treated with propofol (Sigma-Aldrich, St. Louis, MO, USA) in a concentration gradient.

The siRNA against circ_0001727 (si-circ_0001727), miR-516b-5p inhibitor, miR-516b-5p mimic, LRRC1 overexpression plasmid (pc-LRRC1), and corresponding controls (si-NC, inhibitor NC, miRNA NC, and pc-NC) were all synthesized by RiboBio (Guangzhou, China). The oligonucleotide and plasmid were introduced into NSCLC cells (A549 and H1299) by Lipofectamine 3000 Reagent (Invitrogen).

Cell viability assay

Cell Counting Kit-8 (CCK-8) assay was used for analyzing cell viability. Briefly, cell suspension (100 μL) was inoculated into 96-well plates. Following treatment, CCK-8 (10 μL, Bimake, Shanghai, China) was placed into per well for 2–3 h, followed by detection of the optical density (OD) using a microplate reader (Bio-Rad, Hercules, CA, USA) at 450 nm.

RNA isolation and qRT-PCR

After extraction of RNA using TRIzol (Invitrogen), RNA was subjected to reverse transcription with miScript II RT kit (for miRNA; Invitrogen) or PrimeScriptTM RT reagent Kit (for mRNA/circRNA; TaKaRa, Otsu, Japan). Thereafter, qRT-PCR reaction was manipulated using SYBR green PremixEx Taq II (Takara) on Bio-Rad CFX96 system (Bio-Rad). The information of primers was listed: circ_0001727 (F, 5′-CCCAGTCCCACT TCAAACAT-3′; R, 5′-TCAGGCTCCAGGAACTGA CT-3′); ZKSCAN1 (F, 5′-CTCGGAGGAATCTCAGTA GGGA-3′; R, 5′-CGTGATGCTGAATCTTCCGAGG-3′); miR-516b-5p (F, 5′-GCCGAGATCTGGAGGTAA GAA-3′; R, 5′-CAGTGCGTGTCGTGGAGT-3′); LRRC1 (F, 5′-TCCTTACCAAAAGAGATCGG-3′; R, 5′-GGT AGATGCAGCAACCTGT-3′); GAPDH (F, 5′-GTCTCC TCTGACTTCAACAGCG-3′; R, 5′-ACCACCCTGTTG CTGTAGCCAA-3′); U6 (F, 5′-CTCGCTTCGGCAGCA CATATACT-3′; R, 5′-ACGCTTCACGAATTTGCG TGTC-3′). The $2^{-\Delta\Delta Ct}$ method was employed to analyze RNA levels. U6 (for miR-516b-5p) and GAPDH (for

circ_0001727, ZKSCAN1, and LRRC1) were employed as internal controls.

RNase R treatment

RNase R treatment was applied for degrading linear RNA. In brief, total RNA was exposed to RNase R (Duma, Shanghai, China) for half an hour at 37 ℃. After that, circ_0001727 and ZKSCAN1 expression were examined via qRT-PCR.

Colony formation assay

NSCLC cells (A549 and H1299) were seeded into the 6-well plate, and cell culture medium was changed every 3–4 days. After culturing for 2 weeks, these wells were washed and fixed by paraformaldehyde (Beyotime, Jiangsu, China). After staining using crystal violet (Beyotime), these colonies were counted and photographed.

Transwell assay

Transwell assay was used to detect cell migration and invasion. NSCLC cells (A549 and H1299) were suspended in FBS-free medium and plated in the top chamber precoated with (for detecting cell invasion) or without (for detecting cell migration) Matrigel. Meanwhile, completed medium was placed into the bottom chamber. 24 h later, the migrated and invasive cells were fixed in 4% paraformaldehyde (Beyotime) and stained with 0.1% crystal violet solution (Beyotime). Lastly, these cells were photographed by a microscope (× 100, Olympus, Tokyo, Japan).

Tube formation assay

Tube formation assay was carried out to evaluate angiogenesis activity in vitro. When NSCLC cells (A549 and H1299) reached 80% confluence, the supernatant was collected as conditioned medium (CM). Next, human umbilical vein endothelial cells (HUVECs; COBIOER) were inoculated in a 24-well plate coated with Matrigel and incubated for 0.5 h, and then seeded into wells under different CM. After incubation for 6 h in 37 ℃, tube formation was then observed and photographed using a microscope (Olympus). The number of branches in each well was calculated by ImageJ software.

Flow cytometry analysis

Annexin V-FITC&PI apoptosis detection kit purchased form Vazyme was utilized to measure apoptotic cells. Shortly, cells were seeded in 6-well plates and harvested after treatment, followed by resuspending in1 × binding buffer. After staining with Annexin V-FITC and PI for 0.5 h, cells were subjected to a flow cytometer to examine apoptotic cells.

Western blot (WB) assay

After extraction of total protein with RIPA lysis buffer (Vazyme), the total protein was denatured via heating for 3–5 min at 100 ℃. After measurement of protein concentration, total protein was separated by SDS-PAGE. Afterwards, these gels were transferred onto PVDF membranes (Beyotime). After blocking in 5% non-fat milk, these membranes were then probed with the following primary antibodies: vascular endothelial growth factor A (VEGFA; ab51745, 1:1500, Abcam, Cambridge, UK), Bcl-2 (ab194583, 1:1500, Abcam), LRRC1 (HPA031603, 1:1500, Sigma-Aldrich), or GAPDH (ab9485, 1:3000, Abcam) at 4 ℃ for 12–16 h, followed by incubation with secondary antibody (ab205718, 1:5000, Abcam). At last, ECL reagent (Abcam) was used for visualization of protein blots.

Tumor formation assay in vivo

For in vivo assay, we purchased BALB/c nude mice (male, n = 20) from Vital River (Beijing, China) to establish xenograft model and segmented into 2 groups. Short hairpin RNA targeting circ_0001727 (sh-circ_0001727) and sh-NC (as control) were provided by RiboBio. Briefly, mice were subcutaneously inoculated with un-transfected cells (A549) or transfected-cells (sh-circ_0001727 or sh-NC). After injection 7 days, these mice were randomly divided into 4 groups: Control (untreated), propofol, propofol + sh-NC, and propofol + sh-circ_0001727 (n = 5/group). In the propofol groups, propofol (45 mg/kg) was injected intraperitoneally twice a week. An external caliper was used to detect tumor volume. We calculated the volume of tumors according to the equation: $1/2 \times \text{length} \times \text{width}^2$. These mice were sacrificed 4 weeks later, and excised tissues were weighed, followed by collection of the tumor tissues. This study got approval from the Animal Care and Use Committee of the Central Hospital of Enshi Tujia and Miao Autonomous Prefectrue.

Immunohistochemistry (IHC)

Tumor tissues were fixed with paraformaldehyde (4%), embedded in paraffin, and cut at a thickness of 4 μm slides. Next, these sections were incubated with the Ki67 (ab15580, 1:500, Abcam) antibody to measure Ki67 expression. After incubation with secondary antibody (ab171870, 1:2000, Abcam), these sections were then stained using diaminoaniline (DAB; Maxim, Fuzhou, China) and then counterstained using haematoxylin (Maxim). The image was captured using a microscope (Olympus).

Dual-luciferase reporter assay

Circular RNA interactome or starBase was employed to predict the association between miR-516b-5p and circ_0001727 or LRRC1. The fragments of circ_000172 or LRRC1 containing the putative bindings sites for miR-516b-5p were synthesized and cloned into the pmirGLO vectors (GenePharma, Shanghai, China), thereby constructing WT-circ_0001727 or WT-LRRC1-3′UTR. Meanwhile, binding sites for miR-516b-5p were mutated and cloned into the same vector to create MUT-circ_0001727 or MUT-LRRC1-3′UTR. NSCLC cells (A549 and H1299) were co-introduced with the recombinant plasmid and miRNA mimic or miR-516b-5p. 48 h later, the luciferase activities were measured using the dual-luciferase reporter assay system (Promega, Madison, WI, USA).

RNA immunoprecipitation (RIP) assay

RIP assay was conducted with EZ-Magna RIP Kit (Millipore, Billerica, MA, USA). After lysing using RIP buffer, cell lysate (0.1 mL) was incubated with magnetic beads previously binding to human anti-IgG (as the control) or anti-Ago2. The magnetic beads were digested using proteinase K for removing the protein. Lastly, the purified RNA used for measuring the expression of relevant RNAs via qRT-PCR.

Statistical analysis

Data from at least 3 independent experiments displayed as mean ± standard deviation and were analyzed by GraphPad Prism software (Version 7.0). Statistical significance was analyzed via Student's *t* test or a one-way analysis of variance. *P* value < 0.05 was determined to be statistically different.

Results

Propofol inhibited NSCLC cell viability

To investigate the effect of propofol on NSCLC cell viability, NSCLC cells (A549 and H1299) were exposed to various doses of propofol. CCK-8 assay showed that propofol treatment reduced A549 and H1299 cell viability in a dose-dependent way (Fig. 1A, B). Meanwhile, propofol

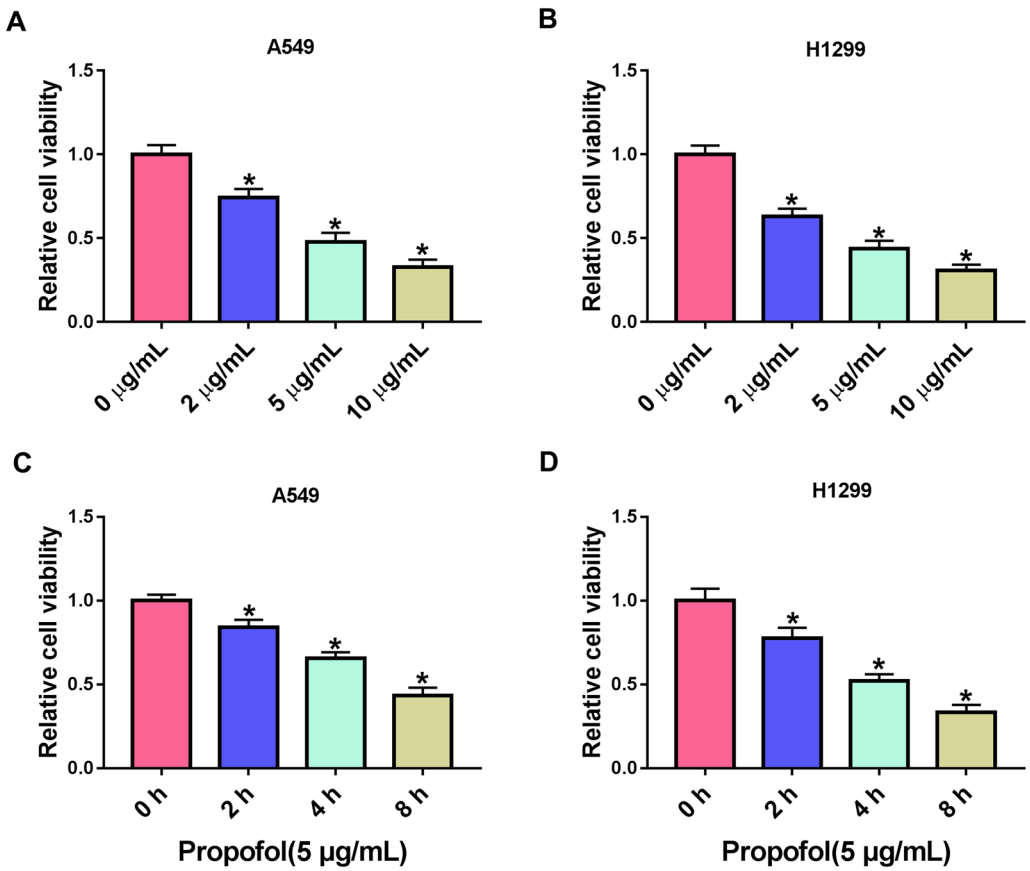

Fig. 1 Propofol suppressed NSCLC cell viability. **A**, **B** CCK-8 assay was used for detection of cell viability in NSCLC cells (A549 and H1299) exposed to various concentrations of propofol. **C**, **D** Cell viability was evaluated in NSCLC cells exposed to propofol for different times. **P* < 0.05.

treatment time-dependently decreased A549 and H1299 cell viability (Fig. 1C, D). Our data indicated that propofol might has an anti-cancer function in NSCLC.

Circ_0001727 was overexpressed in NSCLC

To probe the potential role of circ_0001727 in NSCLC, the expression of circ_0001727 was detected in NSCLC tissues and NSCLC cells. The results showed that circ_0001727 expression was increased in NSCLC tissues relative to adjacent normal tissues (Fig. 2A). Likewise, circ_0001727 level was also enhanced in NSCLC cells (A549 and H1299) (Fig. 2B). Circ_0001727 is generated from the second and third exons of ZKSCAN1 gene and its spliced mature sequence length is 668 bp (Fig. 2C). Generally, RNase R cannot digest circRNAs, but can digest linear RNAs. As presented in Fig. 2D, E, circular isoform (circ_0001727) was resistant to RNase R. Moreover, we found that propofol treatment reduced the expression of circ_0001727 (Fig. 2F). Taken together, circ_0001727 might be associated with NSCLC progression.

Circ_0001727 knockdown increased the anti-cancer role of propofol in NSCLC cells

Since propofol could downregulate the expression of circ_0001727, we further explored whether circ_0001727 participated in propofol-mediated suppression on NSCLC cell progression. Transfection of si-circ_0001727 obviously reduced circ_0001727 level compared to si-NC group (Fig. 3A), indicating a high transfection efficiency. Propofol treatment decreased A549 and H1299 cell viability and colony formation, and combination of circ_0001727 knockdown and propofol led to more obvious inhibition on cell viability and colony-forming ability (Fig. 3B, C). We found similar results of cell viability and colony formation in the propofol group and the propofol + si-NC group, indicating that transfection of si-NC did not influence NSCLC cell behaviors. Angiogenesis can be found in many pathological processes (including the development of most solid tumors) and is a key factor in carcinogenesis. [25, 26]. We found that propofol treatment could reduce migration, invasion, and angiogenesis, and combination of circ_0001727 silence and propofol further decreased cell migration, invasion, angiogenesis compared to only propofol group (Fig. 3D–F). Moreover, circ_0001727 downregulation enhanced propofol-induced apoptosis in NSCLC cells (Fig. 3G). WB assay was carried out to detect the protein levels of VEGFA (one of the important tumor cell-secreted proangiogenic factor) and Bcl-2 (anti-apoptotic molecule). The data showed that propofol suppressed the protein levels of VEGFA and Bcl-2, and circ_0001727 downregulation

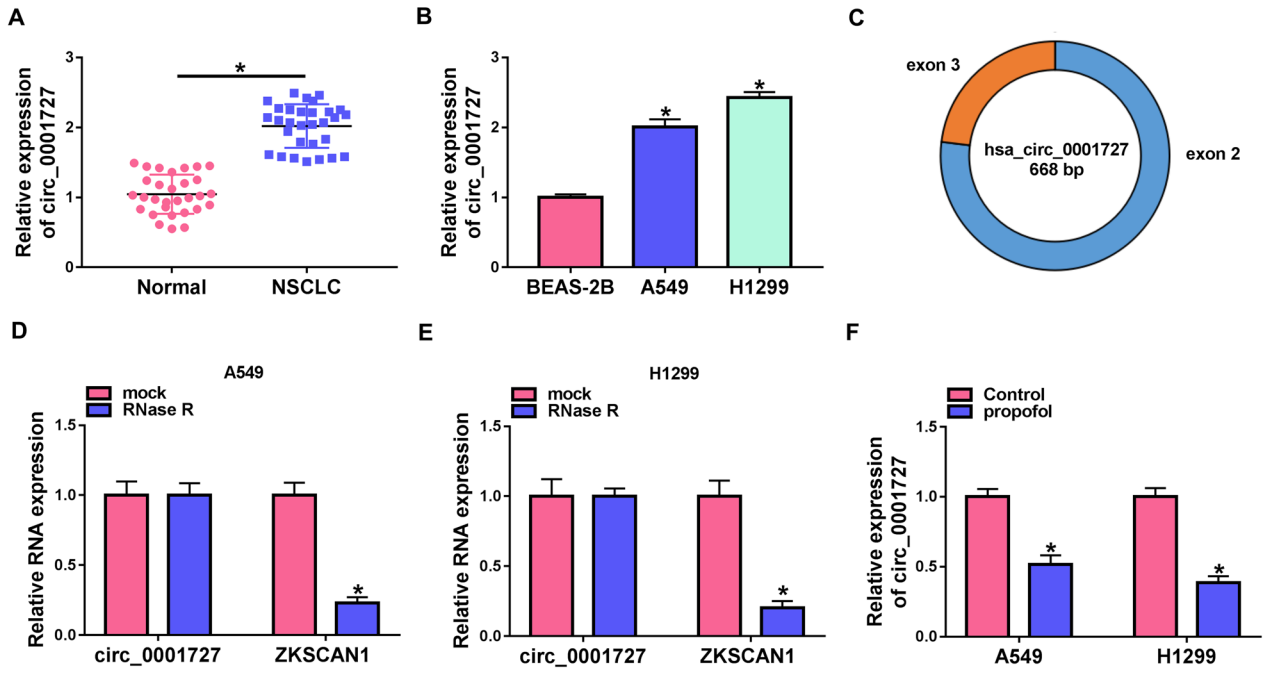

Fig. 2 Circ_0001727 was overexpressed in NSCLC. **A**, **B** Circ_0001727 expression was tested by qRT-PCR in normal tissue samples, NSCLC tissue samples, BEAS-2B cells, and NSCLC cells (A549 and H1299). **C** The information of circ_0001727 was presented. **D**, **E** After treatment of RNase R, circ_0001727 and ZKSCAN1 expression were determined in NSCLC cells. **F** Circ_0001727 expression was determined in NSCLC cells treated with or without propofol. *$P < 0.05$.

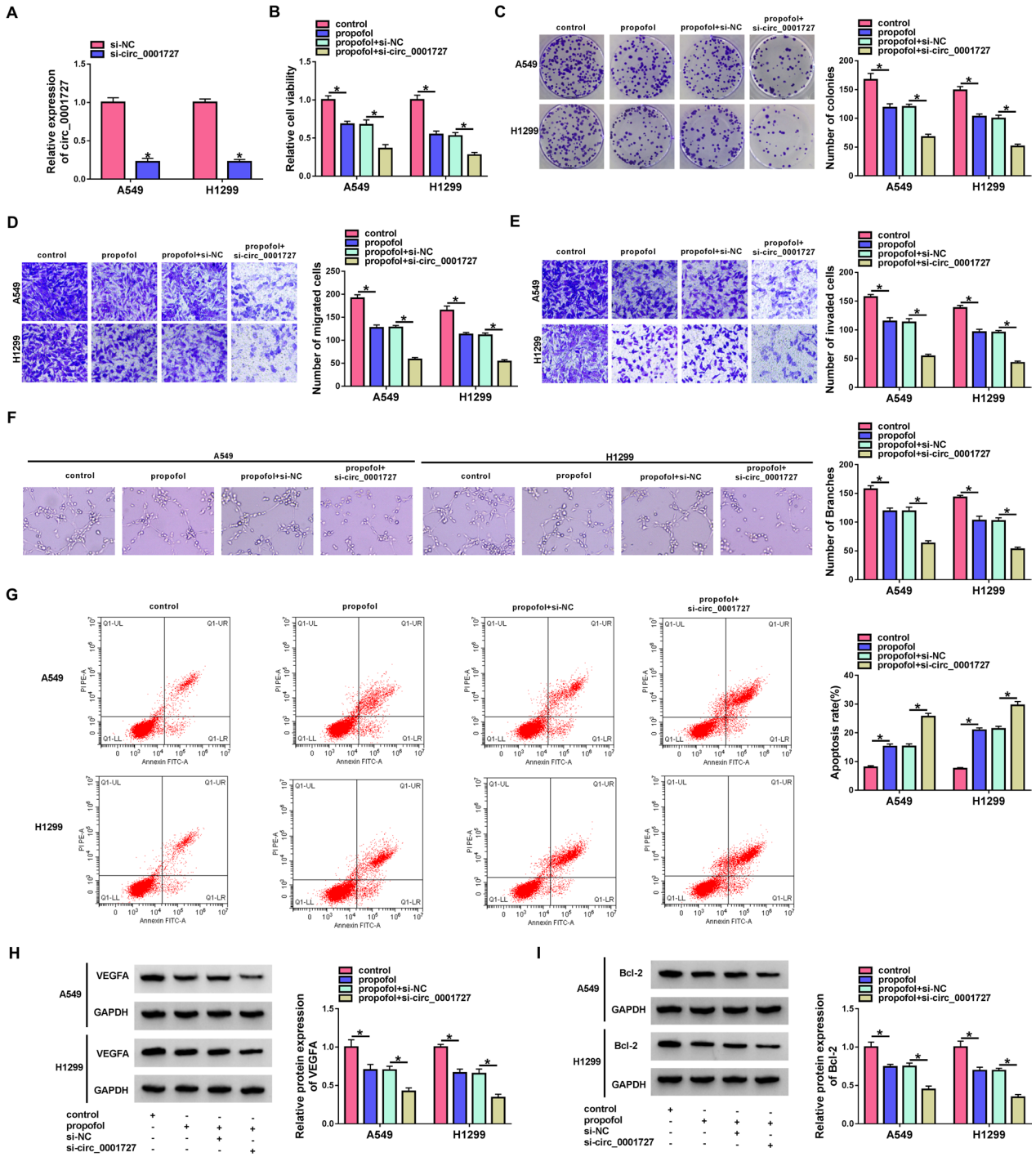

Fig. 3 Propofol limited NSCLC cell malignant behaviors by regulating circ_0001727. **A** Circ_0001727 level was examined in NSCLC cells transfected with si-NC or si-circ_0001727. **B**–**I** NSCLC cells were divided into 4 groups: control group, propofol group, propofol + si-NC group, and propofol + si-circ_0001727 group. **B** CCK-8 analysis was applied for detecting cell viability. **C** Cell colony-forming ability was evaluated by colony formation assay. Cell migration (**D**) invasion (**E**) were evaluated using transwell assay (× 100). **F** Angiogenesis was determined by tube formation assay. **G** Cell apoptosis was detected via flow cytometry. **H**, **I** WB was used to measure the protein expression of VEGFA and Bcl-2. *$P < 0.05$.

together with propofol further inhibited VEGFA and Bcl-2 protein expression (Fig. 3H, I). Taken together, propofol suppressed NSCLC cell progression by regulating circ_0001727.

Circ_0001727 depletion augmented the inhibiting effect of propofol on tumor growth in vivo

To determine the roles of circ_0001727 and propofol in tumor growth in vivo, we established mice xenograft model. Propofol treatment decreased tumor growth (volume and weight), and combination of circ_0001727 knockdown and propofol resulted in more obvious inhibition on tumor growth (Fig. 4A, B). Additionally, propofol treatment inhibited the expression of circ_0001727, and circ_0001727 interference and propofol treatment further inhibited circ_0001727 expression relative to propofol group (Fig. 4C). IHC analysis revealed that circ_0001727 deficiency reduced the expression of Ki67 (a proliferation marker) in tumor tissues, and circ_0001727 depletion in combined with propofol obviously reduced Ki67 expression (Fig. 4D). Collectively, propofol blocked tumor growth in vivo by downregulating circ_0001727.

Circ_0001727 directly targeted miR-516b-5p in NSCLC cells

To elucidate the underlying mechanism of circ_0001727 in NSCLC, the possible miRNA targets of circ_0001727 were predicted by bioinformatics database (circular RNA interactome). We discovered that miR-516b-5p might be a possible target for circ_0001727, and the binding sequence of circ_0001727 in miR-516b-5p and its mutant sites were presented in Fig. 5A. Transfection of miR-516b-5p mimic resulted in a promotion of miR-516b-5p expression in A549 and H1299 cells (Fig. 5B). Overexpressing miR-516b-5p inhibited the luciferase activity of WT-circ_0001727 but not MUT-circ_0001727 (Fig. 5C, D). Meanwhile, circ_0001727 and miR-516b-5p were greatly enriched Ago2 pellets rather than in the IgG control group (Fig. 5E, F), suggesting that Ago2 protein bound to circ_0001727 and miR-516b-5p in NSCLC cells. Next, we detected miR-516b-5p level in NSCLC tissues and cells. MiR-516b-5p expression was both reduced in NSCLC tissues and cells (Fig. 5G, H). Transfection of miR-516b-5p inhibitor obviously reduced miR-516b-5p level, indicating a high inhibition efficiency (Fig. 5I). Moreover, propofol treatment increased miR-516b-5p expression (Fig. 5J). In addition, knockdown of

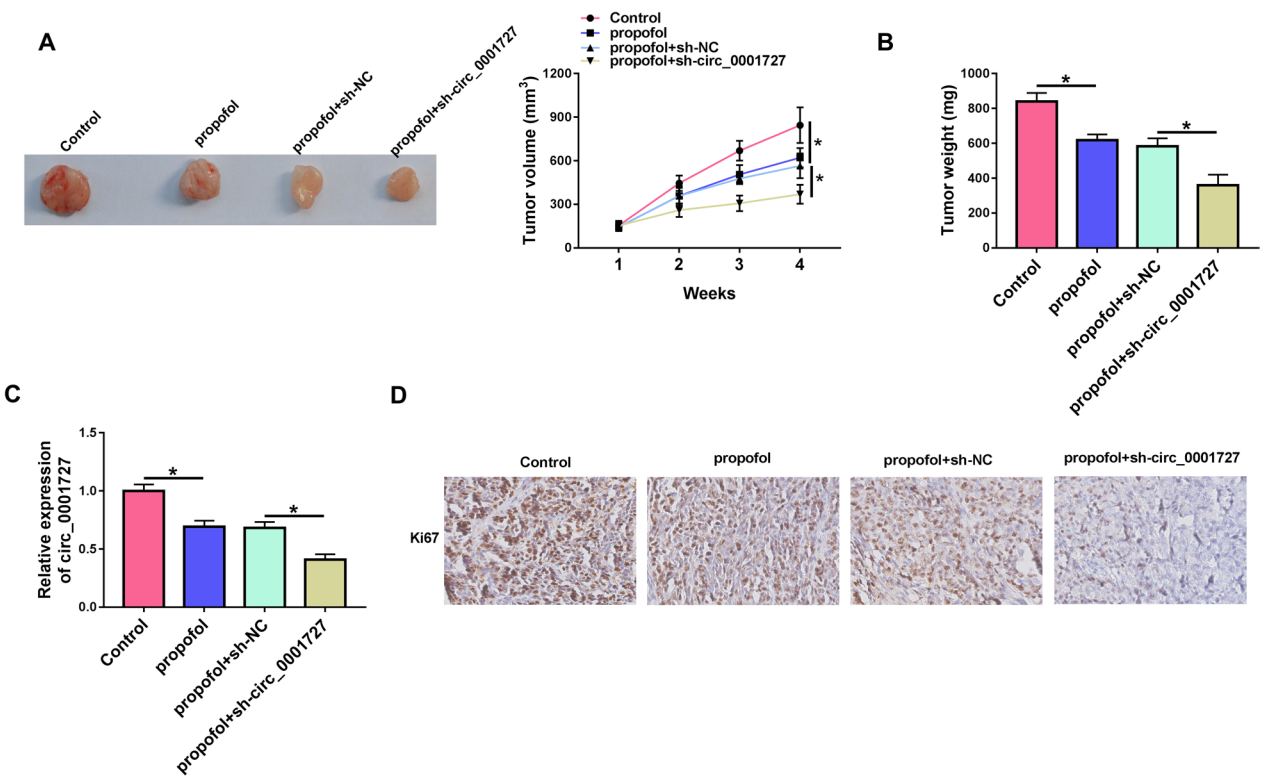

Fig. 4 Circ_0001727 depletion enhanced the repressive impact of propofol on tumor growth in vivo. **A** Representative photographs of tumors were displayed, and tumor volume was recorded every week. **B** Tumor weight was tested following injection for 4 weeks. **C** The abundance of circ_0001727 was examined using qRT-PCR in tumor tissue specimens. **D** Ki67 expression was determined by IHC analysis in tumor tissue specimens. *$P < 0.05$.

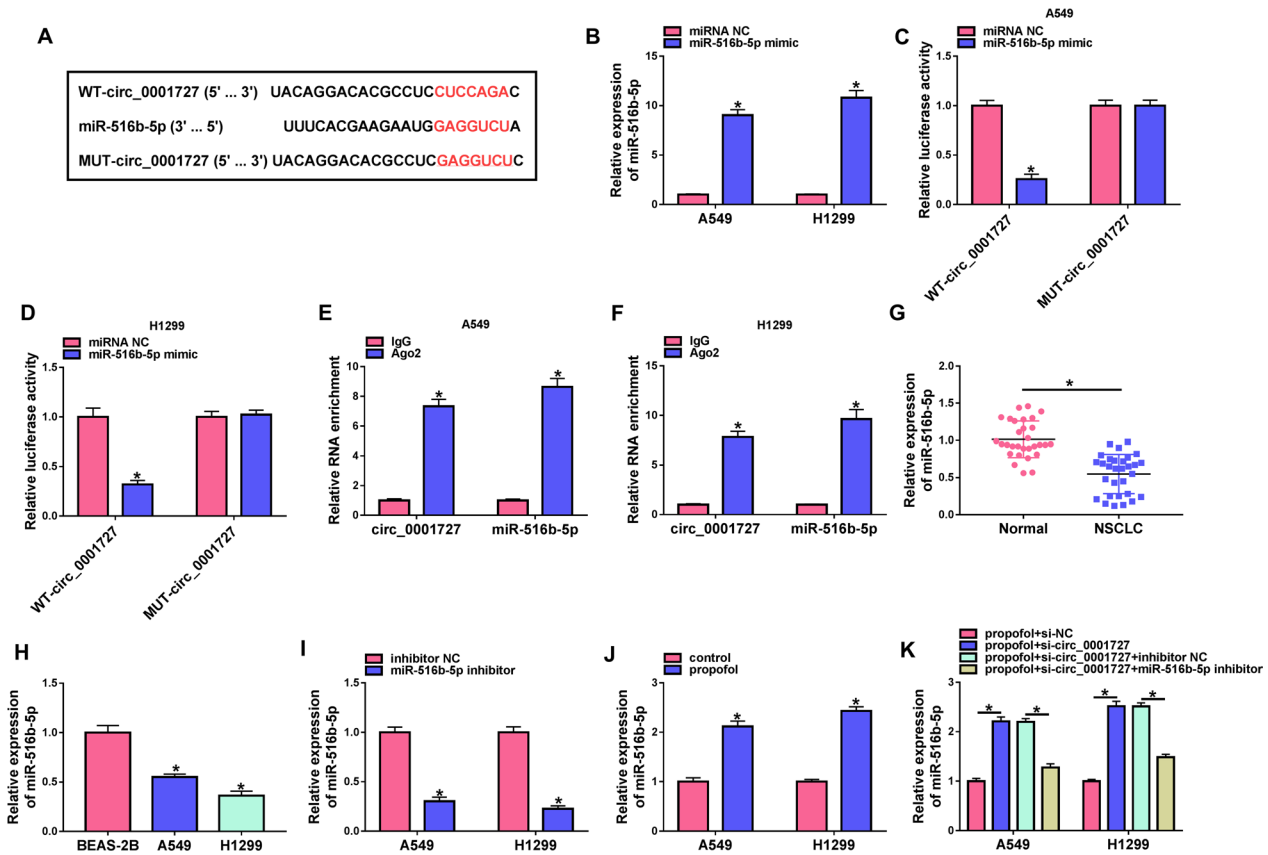

Fig. 5 MiR-516b-5p could directly interact with circ_0001727. **A** The predicted binding sites for circ_0001727 and miR-516b-5p were presented. **B** The expression of miR-516b-5p was detected in NSCLC cells after transfection with miRNA NC or miR-516b-5p mimic. **C**, **D** The luciferase activity in NSCLC cells co-introduced with miRNA NC or miR-516b-5p mimic and WT-circ_0001727 or MUT-circ_0001727 was detected. **E**, **F** Circ_0001727 and miR-516b-5p enrichment were examined in NSCLC cells by RIP assay. **G**, **H** The expression of miR-516b-5p was examined in normal tissue samples, NSCLC tissue samples, BEAS-2B cells, and NSCLC cells. **I** The level of miR-516b-5p was determined in NSCLC cells after transfection with inhibitor NC or miR-516b-5p inhibitor. **J** MiR-516b-5p expression was measured in NSCLC cells treated with or without propofol. **K** MiR-516b-5p abundance was tested in NSCLC cells introduced with si-NC, si-circ_0001727, si-circ_0001727 + inhibitor NC, si-circ_0001727 + miR-516b-5p inhibitor, followed by treatment with propofol. **P* < 0.05.

circ_0001727 enhanced miR-516b-5p expression, which was restored by inhibiting miR-516b-5p in NSCLC cells treated with propofol (Fig. 5K). These results revealed that miR-516b-5p was sponged by circ_0001727.

Circ_0001727 knockdown repressed proliferation, migration, invasion, and angiogenesis and facilitated apoptosis via upregulating miR-516b-5p in propofol-treated NSCLC cells

Subsequently, we explored whether circ_0001727 regulated the behaviors of NSCLC cells via sponging miR-516b-5p. We found that circ_0001727 deficiency reduced cell viability, colony-forming ability, migration, invasion, and angiogenesis, while these inhibitory effects were reversed by downregulating miR-516b-5p in NSCLC cells treated with propofol (Fig. 6A–E). Moreover, circ_0001727 interference increased apoptosis, which was weakened by suppressing miR-516b-5p in propofol-treated NSCLC cells (Fig. 6F). Meanwhile, circ_0001727 downregulation suppressed VEGFA and Bcl-2 protein expression, whereas miR-516b-5p knockdown abated this effect in propofol-treated NSCLC cells (Fig. 6G, H). Together, these results suggested that circ_0001727 knockdown inhibited NSCLC cell progression via sponging miR-516b-5p.

LRRC1 was a direct target for miR-516b-5p

Subsequently, we investigated the downstream targets for miR-516b-5p using starBase. As displayed in Fig. 7A, LRRC1 3'UTR included the binding sequence of miR-516b-5p. The results revealed that miR-516b-5p upregulation led to a decrease in the luciferase activity

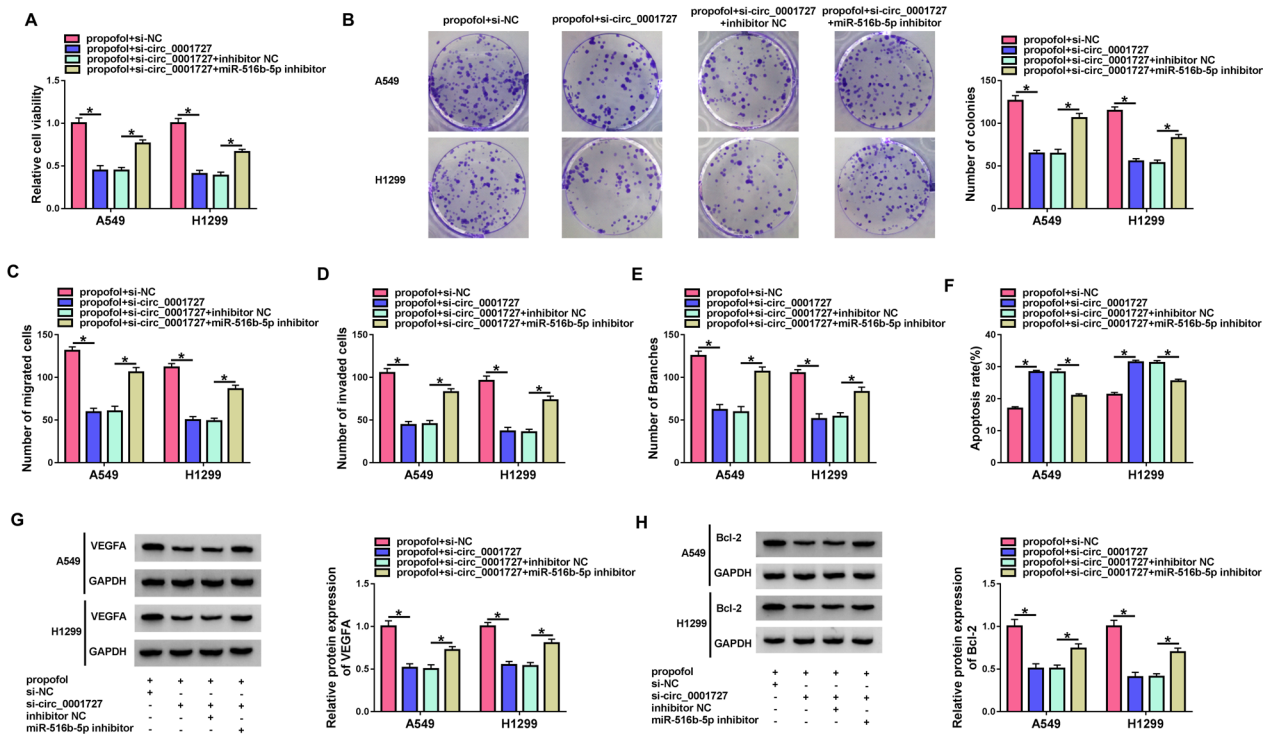

Fig. 6 Downregulation of circ_0001727 inhibited NSCLC cell progression by upregulating miR-516b-5p in propofol-treated NSCLC cells. NSCLC cells were transfected with si-NC, si-circ_0001727, si-circ_0001727 + inhibitor NC, si-circ_0001727 + miR-516b-5p inhibitor, and then treated with propofol. Cell viability (**A**), colony-forming capacity (**B**), migration (**C**), invasion (**D**), angiogenesis (**E**), and cell apoptosis (**F**) were detected. **G**, **H** VEGFA and Bcl-2 protein expression were examined via WB assay. **P* < 0.05.

of WT-LRRC1-3′UTR, while changes in miR-516b-5p expression could not affect the luciferase activity of MUT-LRRC1-3′UTR (Fig. 7B, C). MiR-516b-5p and LRRC1 enrichment were increased in Ago2 group compared to IgG control group (Fig. 7D, E). In NSCLC tissue samples, LRRC1 mRNA and protein levels were increased in comparison with normal tissue samples (Fig. 7F, G). Likewise, LRRC1 protein expression was also enhanced in NSCLC cells (Fig. 7H). Moreover, propofol treatment led to a reduction in LRRC1 protein expression in NSCLC cells (Fig. 7I). LRRC1 was successfully overexpressed in NSCLC cells transfected with pc-LRRC1 (Fig. 7J). In addition, miR-516b-5p overxpression inhibited the protein expression of LRRC1, which was rescued by elevating LRRC1 in NSCLC cells treated with propofol (Fig. 7K). Collectively, miR-516b-5p directly targeted LRRC1.

Restoration of miR-516b-5p suppressed the malignant behaviors of NSCLC cells via targeting LRRC1

Considering that LRRC1 was targeted by miR-516b-5p in NSCLC cells, we further explored whether LRRC1 was implicated in miR-516b-5p-mediated functions in propofol-treated NSCLC cells. Overexpressing miR-516b-5p inhibited cell viability, colony-forming ability, migration, invasion, and angiogenesis, while these suppressive effects were abated by upregulating LRRC1 in NSCLC cells exposed to propofol (Fig. 8A–E). In addition, enforced expression of miR-516b-5p increased cell apoptosis, which could be reversed by increasing LRRC1in propofol-treated NSCLC cells (Fig. 8F). Meanwhile, miR-516b-5p overexpression inhibited VEGFA and Bcl-2 protein expression, which was neutralized by upregulation of LRRC1 in propofol-treated NSCLC cells (Fig. 8G, H). These data revealed that miR-516b-5p played an anti-cancer role in NSCLC cells via downregulation of LRRC1.

Circ_0001727 sponged miR-516b-5p to positively regulate LRRC1 expression

Next, we studied the impact of circ_0001727 and miR-516b-5p on LRRC1 expression in propofol-treated NSCLC cells. The results of WB displayed that circ_0001727 knockdown reduced LRRC1 protein expression, which was restored by inhibition of miR-516b-5p in propofol-treated NSCLC cells (Fig. 9), implying that circ_0001727 serve as a miR-516b-5p sponge to regulate LRRC1 level.

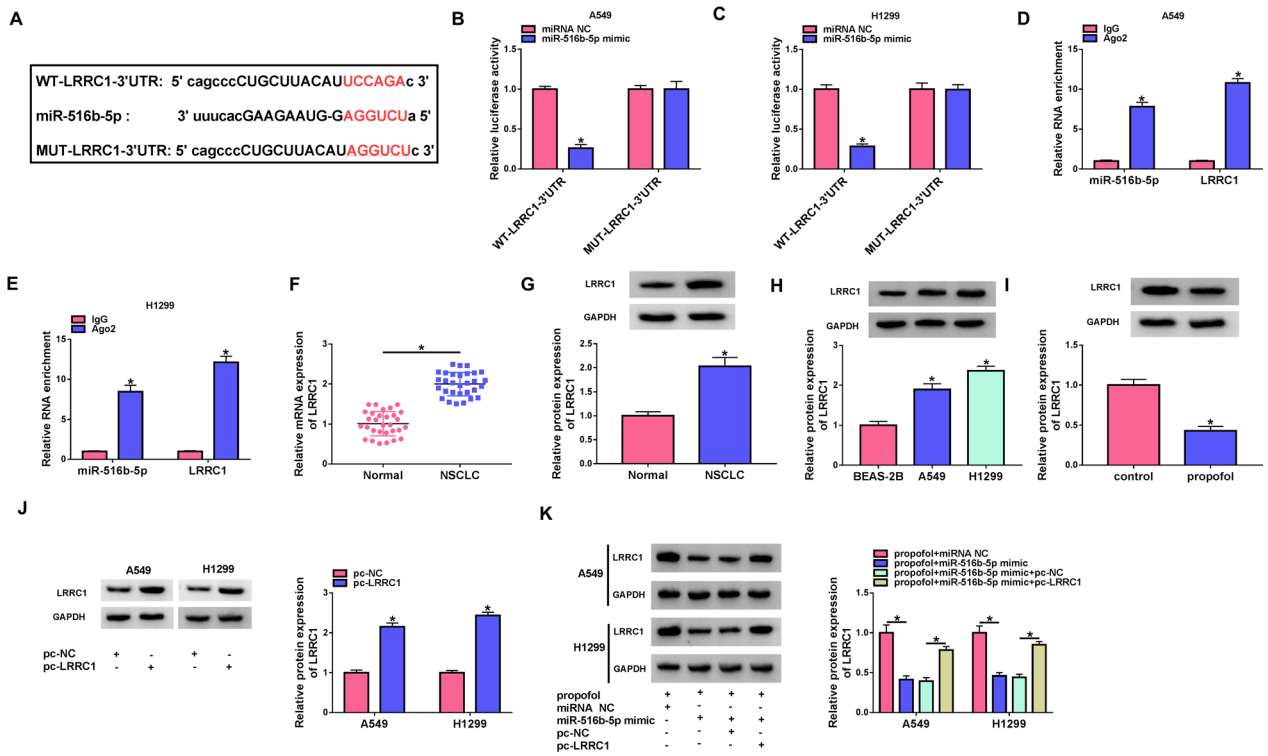

Fig. 7 LRRC1 was directly targeted by miR-516b-5p. **A** The binding sequence of miR-516b-5p and LRRC1 3′UTR was shown. **B**–**E** Dual-luciferase reporter and RIP assays were conducted to confirm the interaction between miR-516b-5p and LRRC1. **F**, **G** LRRC1 mRNA and protein abundance in normal and NSCLC tissues were detected. **H** LRRC1 protein expression was examined by WB in BEAS-2B cells and NSCLC cells. **I** LRRC1 protein expression was analyzed in NSCLC cells treated with or without propofol. **J** LRRC1 protein abundance was detected in NSCLC cells transfected with pc-NC or pc-LRRC1. **K** The expression of LRRC1 protein was determined in NSCLC cells transfected with miRNA NC, miR-516b-5p mimic, miR-516b-5p mimic + pc-NC, or miR-516b-5p mimic + pc-LRRC1, followed by treatment with propofol.

Discussion

Recently, several studies have suggested that propofol possesses anti-tumor, neuroprotective, anti-anxiety, and anti-oxidation roles in several diseases [27–29]. In the current study, propofol facilitated apoptosis while repressed NSCLC cell proliferative ability, mobility, and angiogenesis (in vitro) and also limited tumor growth (in vivo), which was in line with former studies. For example, propofol suppressed NSCLC cell growth and metastasis while accelerated apoptosis via modulating circ-RHOT1/miR-326/FOXM1 axis [30]. Another study demonstrated that propofol restrained lung cancer tumorigenesis through regulating circ-ERBB2/miR-7-5p/FOXM1 network [31].

Propofol can regulate the progression of cancer via various pathways, such as regulating ncRNA expression and serving as a regulator of different signaling pathways [32]. Propofol has been reported to have the anti-tumor function in several cancers through regulation of circRNAs [33, 34]. Hence, we assumed that propofol might inhibit NSCLC progression through regulating other circRNAs. Some studies revealed that circ_0001727 was associated with the development of some cancers, including bladder cancer [35] and hepatocellular carcinoma [36]. Importantly, Wang et al. claimed that circ_0001727 expression was increased in NSCLC, and circ_0001727 reinforced the proliferative ability of NSCLC cells through modulating miR-330-5p/FAM83A axis and inactivating MAPK signaling [19]. According to the above findings, we assumed that propofol might exert its functions via regulating circ_0001727. As expected, propofol treatment could downregulate circ_0001727 expression in NSCLC cells. To investigated whether propofol exerted the anti-tumor function in NSCLC cells by downregulating circ_0001727, we silenced circ_0001727 by transfection with si-circ_0001727 and treated with propofol. We found that circ_0001727 knockdown augmented the anticancer action of propofol in NSCLC cells.

Strikingly, circRNAs commonly serve as miRNA sponges, which result in the decrease of the expression and function of miRNAs [37]. Subsequently, we investigated whether circ_0001727 served as a miRNA sponge. Here, we verified that miR-516b-5p was sponged by circ_0001727. Some researchers have verified the

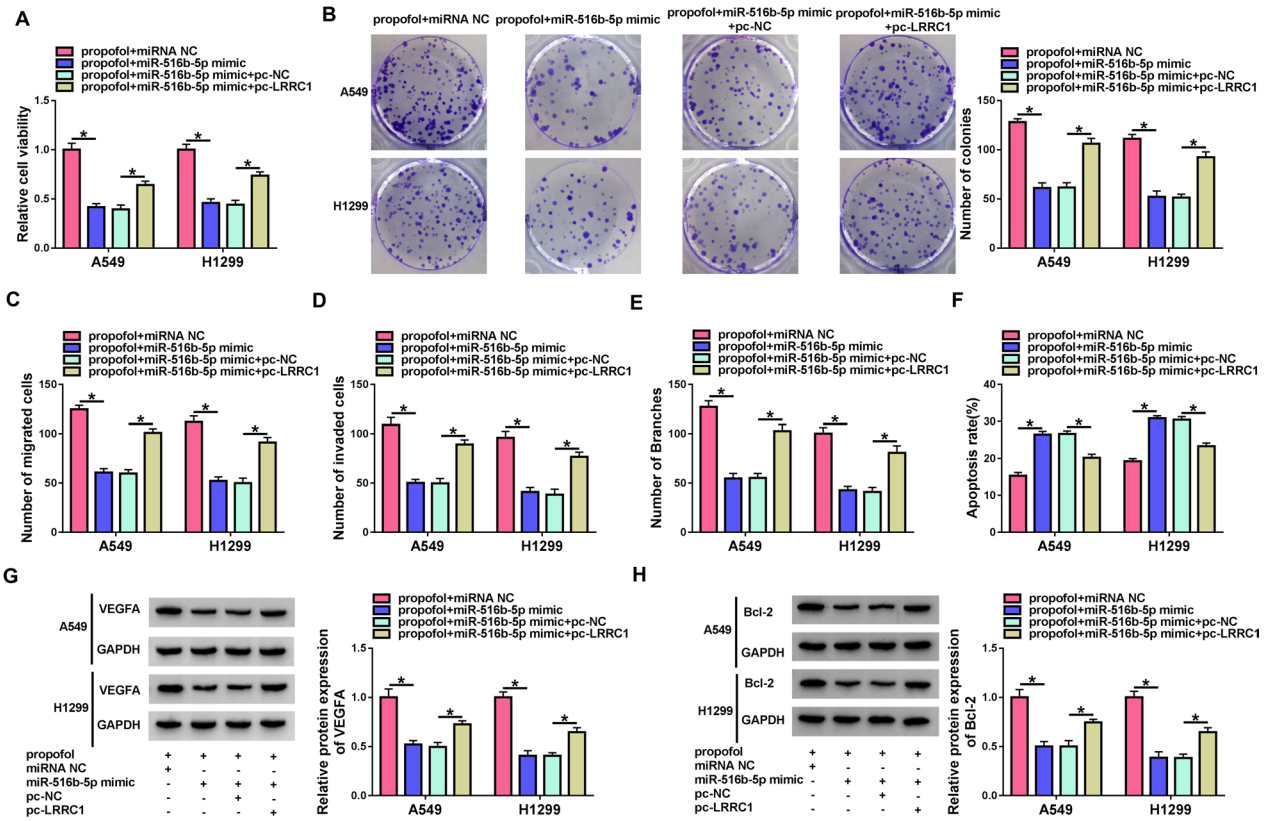

Fig. 8 MiR-516b-5p suppressed NSCLC cell progression via targeting LRRC1 in propofol-treated NSCLC cells. NSCLC cells were transfected with miRNA NC, miR-516b-5p mimic, miR-516b-5p mimic + pc-NC, or miR-516b-5p mimic + pc-LRRC1, followed by exposure to propofol. Cell viability (**A**), colony-forming ability (**B**), migration (**C**), invasion (**D**), angiogenesis (**E**), and cell apoptosis (**F**) were determined. **G**, **H** EGFA and Bcl-2 protein abundance were detected. *$P < 0.05$.

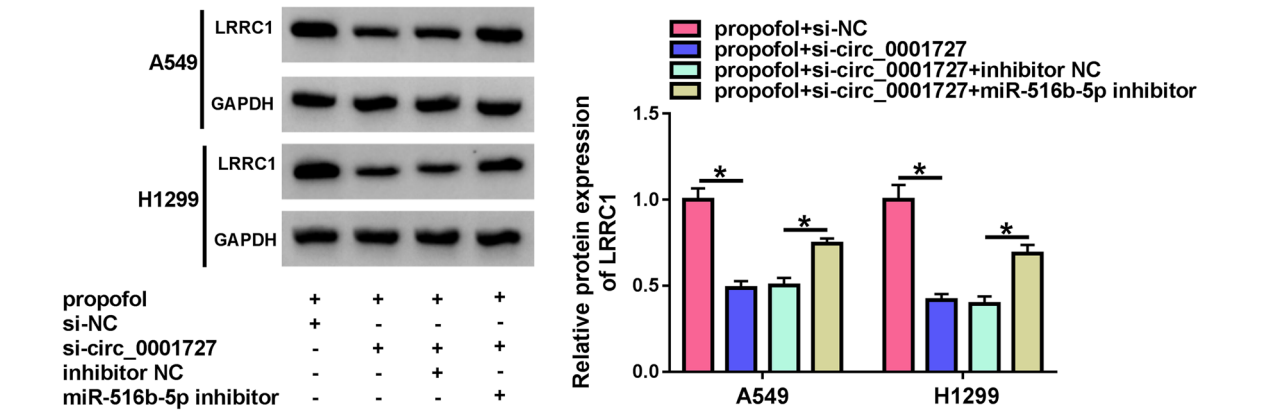

Fig. 9 Circ_0001727 sponged miR-516b-5p to regulate LRRC1 expression. LRRC1 protein abundance was examined by WB in NSCLC cells transfected with si-NC, si-circ_0001727, si-circ_0001727 + inhibitor NC, si-circ_0001727 + miR-516b-5p inhibitor, and then stimulated with propofol. *$P < 0.05$.

anti-tumor role of miR-516b-5p in NSCLC. Xu et al. disclosed that miR-516b-5p level was decreased in NSCLC, and miR-516b-5p inhibition could abolish the suppressive impact of circAKT3 depletion on glycolysis and cisplatin resistance in NSCLC cells [38]. Additionally, Song et al. illustrated that restoration of miR-516b-5p blocked NSCLC cell growth and invasion [23]. In line with this, we uncovered that miR-516b-5p abundance was also declined in NSCLC cell lines and NSCLC tissue specimens. MiR-516b-5p suppression neutralized the inhibiting influence of circ_0001727 depletion on NSCLC cell progression, suggesting that propofol inhibited NSCLC cell progression via regulation of circ_0001727/miR-516b-5p axis.

MiRNAs exert their functions via regulating the expression of target mRNAs [39]. Based on bioinformatics analysis and a series of experiments, LRRC1 was demonstrated to be directly targeted by miR-516b-5p. A previous has demonstrated that LRRC1 can promote the development of hepatocellular carcinoma [40]. Moreover, LRRC1 was demonstrated to be upregulated in NSCLC, and knockdown of LRRC1 repressed NSCLC cell invasion, proliferation and migration and accelerated apoptosis [24]. In this study, LRRC1 was overexpressed in NSCLC tissues and cells. However, propofol treatment reduced LRRC1 expression in NSCLC cells. Rescue experiments showed that LRRC1 overexpression counteracted the anti-tumor role of miR-516b-5p on in NSCLC cells, indicating that miR-516b-5p regulated NSCLC cell behaviors by targeting LRRC1. Mechanistically, circ_0001727 regulated LRRC1 expression via sponging miR-516b-5p in propofol-exposed NSCLC cells.

In conclusion, propofol could suppress NSCLC progression via regulating the circ_0001727/miR-516b-5p/LRRC1 network. These results might offer an effective therapeutic target for NSCLC.

Acknowledgements
None.

Author contributions
MT designed the study, analyzed the data and wrote the manuscript. XZ performed the experiments. MX analyzed the data. All authors read and approved the final manuscript.

Funding
There is no funding to report.

Availability of data and materials
All data generated or analysed during this study are available in this article.

Declarations

Ethics approval and consent to participate
The design of this protocol follows the tenets of the Declaration of Helsinki, approved by the Ethics Committee of the Central Hospital of Enshi Tujia and Miao Autonomous Prefectrue.

Competing interests
The authors declare that they have no competing interests.

Author details
[1]Department of Tumor Diagnosis and Treatment Center of Chinese and Western mtegrative Medicine, The Central Hospital of Enshi Tujia and Miao Autonomous Prefectrue, Enshi City, Hubei, China. [2]Department of Oncology, The Central Hospital of Enshi Tujia and Miao Autonomous Prefectrue, No. 156 Wuyang Avenue, Enshi City 445000, Hubei, China.

Received: 24 December 2021 Accepted: 21 March 2022
Published online: 04 April 2022

References

1. Sung H, Ferlay J, Siegel RL et al (2021) Global cancer statistics 2020: GLOBOCAN estimates of incidence and mortality worldwide for 36 cancers in 185 countries. CA Cancer J Clin 71(3):209–249
2. Gridelli C, Rossi A, Carbone DP et al (2015) Non-small-cell lung cancer. Nat Rev Dis Prim 1:15009
3. Hirsch FR, Suda K, Wiens J, Bunn PA Jr (2016) New and emerging targeted treatments in advanced non-small-cell lung cancer. Lancet 388(10048):1012–1024
4. Chidambaran V, Costandi A, D'Mello A (2015) Propofol: a review of its role in pediatric anesthesia and sedation. CNS Drugs 29(7):543–563
5. Qi Z, Yuan L, Sun N (2019) Propofol exhibits a tumor-suppressive effect and regulates cell viability, migration and invasion in bladder carcinoma by targeting the microRNA-10b/HOXD10 signaling pathway. Oncol Lett 18(6):6228–6236
6. Yu X, Gao Y, Zhang F (2019) Propofol inhibits pancreatic cancer proliferation and metastasis by up-regulating miR-328 and down-regulating ADAM8. Basic Clin Pharmacol Toxicol 125(3):271–278
7. Fei G, Cao M, Ge C, Cui L (2020) Propofol suppresses hepatocellular carcinoma by inhibiting NET1 through downregulating ERK/VEGF signaling pathway. Sci Rep 10(1):11208
8. Li Y, Dong W, Yang H, Xiao G (2020) Propofol suppresses proliferation and metastasis of colorectal cancer cells by regulating miR-124–3p.1/AKT3. Biotechnol Lett 42(3):493–504
9. Wu X, Li X, Xu G (2020) Propofol suppresses the progression of non-small cell lung cancer via downregulation of the miR-21-5p/MAPK10 axis. Oncol Rep 44(2):487–498
10. Geng Y, Jiang J, Wu C (2018) Function and clinical significance of circRNAs in solid tumors. J Hematol Oncol 11(1):98
11. Chen L-L, Yang L (2015) Regulation of circRNA biogenesis. RNA Biol 12(4):381–388
12. Li X, Yang L, Chen LL (2018) The biogenesis, functions, and challenges of circular RNAs. Mol Cell 71(3):428–442
13. Zhang Y, Xue W, Li X et al (2016) The biogenesis of nascent circular RNAs. Cell Rep 15(3):611–624
14. Shang Q, Yang Z, Jia R, Ge S (2019) The novel roles of circRNAs in human cancer. Mol Cancer 18(1):6
15. Zhang Z, Yang T, Xiao J (2018) Circular RNAs: promising biomarkers for human diseases. EBioMedicine 34:267–274
16. Zhang N, Nan A, Chen L et al (2020) Circular RNA circSATB2 promotes progression of non-small cell lung cancer cells. Mol Cancer 19(1):101
17. Chen T, Yang Z, Liu C et al (2019) Circ_0078767 suppresses non-small-cell lung cancer by protecting RASSF1A expression via sponging miR-330-3p. Cell Prolif 52(2):e12548
18. Li X, Yang B, Ren H et al (2019) Hsa_circ_0002483 inhibited the progression and enhanced the Taxol sensitivity of non-small cell lung cancer by targeting miR-182-5p. Cell Death Dis 10(12):953
19. Wang Y, Xu R, Zhang D et al (2019) Circ-ZKSCAN1 regulates FAM83A expression and inactivates MAPK signaling by targeting miR-330-5p to promote non-small cell lung cancer progression. Transl Lung Cancer Res 8(6):862–875
20. Ardekani AM, Naeini MM (2010) The role of microRNAs in human diseases. Avicenna J Med Biotechnol 2(4):161–179
21. Lee YS, Dutta A (2009) MicroRNAs in cancer. Annu Rev Pathol 4:199–227
22. Hansen TB, Jensen TI, Clausen BH et al (2013) Natural RNA circles function as efficient microRNA sponges. Nature 495(7441):384–388

23. Song H, Li H, Ding X et al (2020) Long non-coding RNA FEZF1-AS1 facilitates non-small cell lung cancer progression via the ITGA11/miR-516b-5p axis. Int J Oncol 57(6):1333–1347
24. Wu H, Mu X, Liu L et al (2020) Bone marrow mesenchymal stem cells-derived exosomal microRNA-193a reduces cisplatin resistance of non-small cell lung cancer cells via targeting LRRC1. Cell Death Dis 11(9):801
25. Carmeliet P, Jain RK (2000) Angiogenesis in cancer and other diseases. Nature 407(6801):249–257
26. Bagnasco L, Piras D, Parodi S et al (2012) Role of angiogenesis inhibitors in colorectal cancer: sensitive and insensitive tumors. Curr Cancer Drug Targets 12(4):303–315
27. Ulbrich F, Eisert L, Buerkle H, Goebel U, Schallner N (2016) Propofol, but not ketamine or midazolam, exerts neuroprotection after ischaemic injury by inhibition of Toll-like receptor 4 and nuclear factor kappa-light-chain-enhancer of activated B-cell signalling: A combined in vitro and animal study. Eur J Anaesthesiol 33(9):670–680
28. Tian Y, Guo S, Guo Y, Jian L (2015) Anesthetic propofol attenuates apoptosis, Aβ accumulation, and inflammation induced by sevoflurane through NF-κB pathway in human neuroglioma cells. Cell Mol Neurobiol 35(6):891–898
29. Su Z, Hou XK, Wen QP (2014) Propofol induces apoptosis of epithelial ovarian cancer cells by upregulation of microRNA let-7i expression. Eur J Gynaecol Oncol 35(6):688–691
30. Zhang Q, Cheng F, Zhang Z, Wang B, Zhang X (2021) Propofol suppresses non-small cell lung cancer tumorigenesis by regulation of circ-RHOT1/miR-326/FOXM1 axis. Life Sci. https://doi.org/10.1016/j.lfs.2021.119042
31. Gao J, Ding C, Zhou J et al (2021) Propofol suppresses lung cancer tumorigenesis by modulating the circ-ERBB2/miR-7-5p/FOXM1 axis. Thorac Cancer 12(6):824–834
32. Jiang S, Liu Y, Huang L, Zhang F, Kang R (2018) Effects of propofol on cancer development and chemotherapy: potential mechanisms. Eur J Pharmacol 831:46–51
33. Sui H, Zhu C, Li Z, Yang J (2020) Propofol suppresses gastric cancer tumorigenesis by modulating the circular RNA-PVT1/miR-195-5p/E26 oncogene homolog 1 axis. Oncol Rep 44(4):1736–1746
34. Zhao H, Wei H, He J et al (2020) Propofol disrupts cell carcinogenesis and aerobic glycolysis by regulating circTADA2A/miR-455-3p/FOXM1 axis in lung cancer. Cell Cycle 19(19):2538–2552
35. Bi J, Liu H, Dong W et al (2019) Circular RNA circ-ZKSCAN1 inhibits bladder cancer progression through miR-1178-3p/p21 axis and acts as a prognostic factor of recurrence. Mol Cancer 18(1):133
36. Li J, Bao S, Wang L, Wang R (2021) CircZKSCAN1 suppresses hepatocellular carcinoma tumorigenesis by regulating miR-873-5p/downregulation of deleted in liver cancer 1. Dig Dis Sci 66(12):4374–4383
37. Panda AC (2018) Circular RNAs act as miRNA sponges. Adv Exp Med Biol 1087:67–79
38. Xu Y, Jiang T, Wu C, Zhang Y (2020) CircAKT3 inhibits glycolysis balance in lung cancer cells by regulating miR-516b-5p/STAT3 to inhibit cisplatin sensitivity. Biotechnol Lett 42(7):1123–1135
39. Felekkis K, Touvana E, Stefanou C, Deltas C (2010) microRNAs: a newly described class of encoded molecules that play a role in health and disease. Hippokratia 14(4):236
40. Li Y, Zhou B, Dai J, Liu R, Han ZG (2013) Aberrant upregulation of LRRC1 contributes to human hepatocellular carcinoma. Mol Biol Rep 40(7):4543–4551

Publisher's Note